Hindawi
Mathematical Problems in Engineering
Volume 2019, Article ID 1458149, 14 pages
https://doi.org/10.1155/2019/1458149

Research Article

Path Contribution Analysis of Vibration Transfer Path Systems

Wei Zhao,[1] **Yi-Min Zhang**,[1] **and Wen-Zhou Feng**[2]

[1]*School of Mechanical Engineering and Automation, Northeastern University, Shenyang 110819, China*
[2]*School of Mechanical Engineering, Tianjin University, Tianjin 300350, China*

Correspondence should be addressed to Wei Zhao; weizhao@mail.neu.edu.cn

Received 11 August 2018; Revised 20 November 2018; Accepted 18 December 2018; Published 8 January 2019

Academic Editor: Xiao-Qiao He

Copyright © 2019 Wei Zhao et al. This is an open access article distributed under the Creative Commons Attribution License, which permits unrestricted use, distribution, and reproduction in any medium, provided the original work is properly cited.

To analyze the vibration characteristics of mechanical systems from the aspect of vibration transfer, two types of models for vibration transfer path systems were designed, which comprised three subsystems: excitation sources, transfer paths, and receivers. One type of model represented that the systems only sustained unidirectional force excitation, where the transfer paths remained free from the influence of mass parameters. The other type indicated that the systems were subjected to simultaneous excitations of forces and moments, with transfer paths without mass parameter. Because the transfer characteristics of vibration paths directly determine the output response behaviours of the systems, the analysis of path contributions to the vibration responses of system receivers is important in systemic vibration and noise reduction. In order to evaluate the path contributions quantitatively, the concepts of path transfer ratio (TR) and path insertion loss (IL) were introduced and the convenient formulae were derived based on the path transfer force analysis and the path disconnected method in this work. Thereby the measurement of path contributions to the receiver vibration responses within the frequency domain can be accomplished. Through numerical examples, the ideal calculation results were obtained. These conclusions further indicate that the path TR and path IL can be applied as evaluation indicators of path contributions for the vibration transfer path systems.

1. Introduction

Vibration and noise performance has long remained the main aspect for evaluating the quality of mechanical equipment. Particularly, with the steadily increasing social productivity, the performance of various mechanical equipment exhibits a trend towards high velocity, lightweight, and heavy duty features. Therefore, engineers are required to continuously address vibration control problems. In order to achieve the desired design requirements, the vibration control problem should be largely addressed from the following three aspects: the identification of vibration sources, the optimization of transfer paths, and the vibration elimination of receivers [1, 2]. The technique of vibration source identification is mainly based on the measurement of normal vibration velocity on the source surface and the near-field acoustic pressure measurement. The accuracy can be largely influenced by the environment factors, the sensor location, and the sensor amount [3, 4]. The vibration elimination of receiver is the passive control for the output vibration. The application of dynamic vibration absorber is most common, but it is limited to a certain frequency range. The nonlinear vibration absorber has the characteristics of wide frequency absorption, but because of its complex structure, it is difficult to be applied in practice [5, 6]. By comparison, vibration isolation and structural dynamic optimization remain an effective approach for vibration control. Moreover, the dynamic optimization technique could be guaranteed in the early stage of system design based on the specific analyses of transfer paths in a vibration system [7, 8].

For the problem of path transitivity, the current research includes the transfer path analysis (TPA) of test-based methodologies and statistical energy analysis. The TPA is more used to deal with the low-frequency problems [9, 10]. Moreover, for the purpose of operability and saving time in the experiments, this method usually departs from the traditional source-transfer-receiver model with the assumption of the loads with physical meanings, frequency response function, and the partial response [11, 12]. For example, D. de Klerk and A. Ossipov et al. provided the operational transfer path analysis (OTPA), whose simple and fast modeling is the biggest advantage [13, 14]. Ba-Leum Kim and Yoshida J

et al. developed the modified transfer path analysis (MTPA) method to more accurately estimate the operational force of the main vibration source in a complicated system subjected to multiple vibration sources, base excitation, and several disturbances [15]. Therefore, the accuracy of the experimental results must be affected to a certain extent. Hou Lei and Zhang Jiming measured the response of each installation point and evaluation point and the excitation force. According to the frequency response function, the transfer path analysis was completed, and the contributions of equipment and pipeline were obtained [16]. However, since the direct measurement of the excitation force is almost impossible, the excitation force can only be obtained through the admittance characteristics of the installation system. Additionally, the ill-conditioned problem of matrix inversion may affect the accuracy of pipeline contribution to a certain extent. The statistical energy analysis can solve the dynamics problems in high-frequency domains for the complex systems. Due to the large workload, the practical application of this analytical method to the complex systems is very limited. Many researchers usually use the mobility power flow theory to solve the practical problems [17–19]. In fact, the power flow method is only applicable to the modeling and analysis of vibration system in the middle and low-frequency bands. Xiao Bin and Li Biao et al. established vibration energy model of double-layer vibration isolation system based on power flow method. The corresponding vibration transmission was studied combined with vibration isolation system test and modal test [20]. The two research methods mentioned above mainly depend on the support of various experimental methods and the research for the prediction of vibration characteristics is limited.

Generally, there are multiple vibration transfer paths in practical mechanical vibration systems. Each path not only has the effect for vibration transferring, but also affects the dynamic characteristics of the whole system. From these two aspects, this work applied two evaluation indicators to analyze path contributions in the vibration transfer path systems, namely, the path transfer ratio (TR) and insertion loss (IL). Based on the path transfer force analysis and the path disconnected method, the quantitative analysis method could be further employed to investigate the ranking problem with respect to path contributions in the frequency domain. Moreover, this method can be applied to a wider frequency range and could conveniently and effectively identify the critical path. Hence, this could truly solve the problem of low-vibration and low-noise design.

2. Evaluation Indicators of Path Contribution

2.1. Path Transfer Ratio. For the vibration transfer path systems, the transfer capacity of each path is different due to the differences in path structure and path parameters. In order to quantitatively evaluate the contribution of each path to the receiver vibration, we give the concept of path transfer ratio, that is, the ratio between the force to the receiver and the excitation force of the source.

In order to make the analysis process more concise and clear, we assume the vibration transfer path system is excited by the harmonic force $F_0 \sin \omega t$ and there is a fixed connection between a path and a receiver. According to the traditional theory of vibration mechanics analysis and the definition of path force [21], the force that is transferred to the receiver through the path is

$$F_T = |kx + c\dot{x}| \tag{1}$$

where k is spring stiffness and c is damping coefficient.

Based on the calculation method of force transmissibility in the vibration isolation systems [22], the calculation formula of the corresponding path TR is

$$TR = \frac{F_T}{F_0} \tag{2}$$

It can be seen that the path TR is a simple and quick evaluation indicator to analyze the path contribution, which can be used as the theoretical prediction basis for the path transitivity.

2.2. Insertion Loss. The concept of IL was initially applied in electronic systems, where it was defined as the ratio of the power that was transferred to the load with a certain component to the power transferred to the load without the certain component. It was normally quantified using the unit of decibel (dB), expressed as

$$IL = 20 \lg \left(\frac{v1}{v2} \right) \tag{3}$$

where v1 and v2 denote the power before and after an electronic component is connected to the system, respectively [23, 24].

In this work, this concept was introduced into the vibration transfer path system. When analyzing the path contribution, the path IL could be defined based on the ratio of the receiver responses prior to and after the connection of a certain transfer path.

Evidently, a high path IL indicated the high contribution of the path in the vibration transfer system. According to the varying responses of selected receiver, the ILs could be classified into displacement IL, velocity IL, and acceleration IL.

According to the definition, the calculation formula of velocity IL may be written as

$$IL_v(\omega) = 20 \lg \left| \frac{\dot{x}_o}{\dot{x}_{all}} \right| \tag{4}$$

where $\dot{x}_o$ denotes the velocity response of the receiver prior to the path connection, while $\dot{x}_{all}$ represents that of the receiver after the path connection.

Similarly, (4) may be expressed as

$$\begin{aligned} IL_v(\omega) &= 10\lg\frac{\left|\dot{x}_o\right|^2}{\left|\dot{x}_{all}\right|^2} = 10\lg\left|\dot{x}_o\right|^2 - 10\lg\left|\dot{x}_{all}\right|^2 \\ &= \left(10\lg\left(\frac{1}{2}m\right) + 10\lg\left|\dot{x}_o\right|^2\right) \\ &\quad - \left(10\lg\left(\frac{1}{2}m\right) + 10\lg\left|\dot{x}_{all}\right|^2\right) \\ &= 10\lg\left(\frac{1}{2}m\left|\dot{x}_o\right|^2\right) - 10\lg\left(\frac{1}{2}m\left|\dot{x}_{all}\right|^2\right) \\ &= 10\lg\left|\frac{E_o}{E_{all}}\right| \end{aligned} \tag{5}$$

where m is the mass of the receiver, E_o denotes the energy of the receiver prior to path connection, and E_{all} is the energy of the receiver after the path connection.

Hence, the formula for the calculation of energy IL could be expressed as follows:

$$IL_E(\omega) = 10\lg\left|\frac{E_o}{E_{all}}\right| \tag{6}$$

When a receiver is characterized by a coupled rectilinear and swaying motion, to avoid the biased consideration of the path transfer in a single direction, energy IL is generally adopted to assess the importance of the paths.

3. Vibration Transfer Path System Model

In engineering practices, many mechanical vibration systems are established with multiple vibration transfer paths. For example, with respect to a vehicle powertrain subsystem, the excitations generated by the operating engine are transferred to the vehicle body via the three-point suspension system; thereby the vibrations of the vehicle body are induced [25]. The function of the suspension subsystem in the powertrain system is to attenuate the vibration energy transmitted to the vehicle body, so it is a vibration isolation system. At the same time, this subsystem is also a dynamic vibration absorption system for the whole vehicle, which can alleviate the impact of road roughness to the car body. These require that the suspension system should have large stiffness and damping to prevent excessive displacement of power plant when subjected to low-frequency impact and low stiffness and small damping to ensure comfort when subjected to high-frequency vibration. Therefore, when designing suspension system, it is necessary to optimize the parameter matching of damping and stiffness in order to obtain the best vibration transmission performance. Path contribution analysis can find out the critical path, determine the direction for optimization design, and then improve work efficiency. These vibration transfer paths have been described without any mass parameter, so we can make use of the system model shown in Figure 1 to analyze the path contributions.

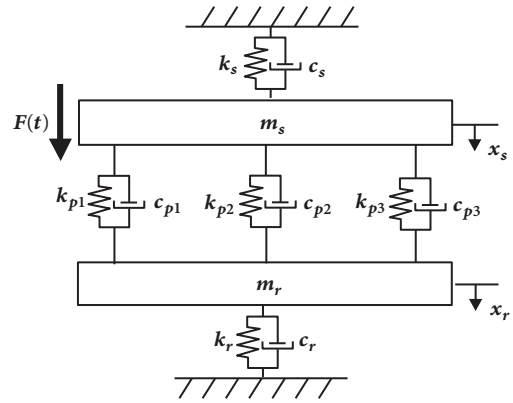

Figure 1: Vibration transfer path system model with linear motion.

This model has three transfer paths parallel to each other and the paths include two types of physical parameters: stiffness and damping. k_{p1}, k_{p2}, and k_{p3} denote the path stiffness, respectively, while c_{p1}, c_{p2}, and c_{p3} represent the path damping respectively. m_s is the mass of the vibration source. k_s is the stiffness for the fixed end of vibration source and c_s is the corresponding damping. Besides, the receiver mass is m_r, and the stiffness for the fixed end of the receiver is k_r with the damping c_r. Here, only single-excitation is considered. The vibration source is subjected to a vertical force excitation $F_0 \sin \omega t$. Thus, the vibration source and receiver only have the linear motion.

For most of the general vibration systems, the model shown in Figure 1 can describe entirely the path transfer characteristics and bring great convenience to theoretical calculations. As for the complex vibration systems, we need to give the corresponding vibration transfer path system model based on the basic model shown in Figure 1. For the vessel system, three sets of bearing pedestal structures between the vessel body and the propulsion shaft system act as the vibration transfer path subsystem. Moreover, when excited by the propulsion shaft system, the vessel body is subjected to the force (moment) that is transferred from the intermediate path; thereby the corresponding vibration responses are produced [26, 27]. The mounting positions of bearing pedestal have great influence on the vibration transmission to the vessel body and the mass, stiffness, and damping characteristics of bearing pedestal interact with their mounting positions to determine the path contributions of vibration transmission. Therefore, when designing this kind of vibration system, not only path physical parameters such as mass, stiffness, and damping should be optimized, but also path geometric parameters such as shape and location should be optimized. In order to achieve the low-vibration design for these kinds of mechanical systems, the vibration transfer path system model shown in Figure 2 is proposed.

The transfer paths shown in Figure 2 encompass not only stiffness and damping, but also path mass. As compared to the vibration transfer path system without path mass, the vibration system with mass parameters in transfer paths is

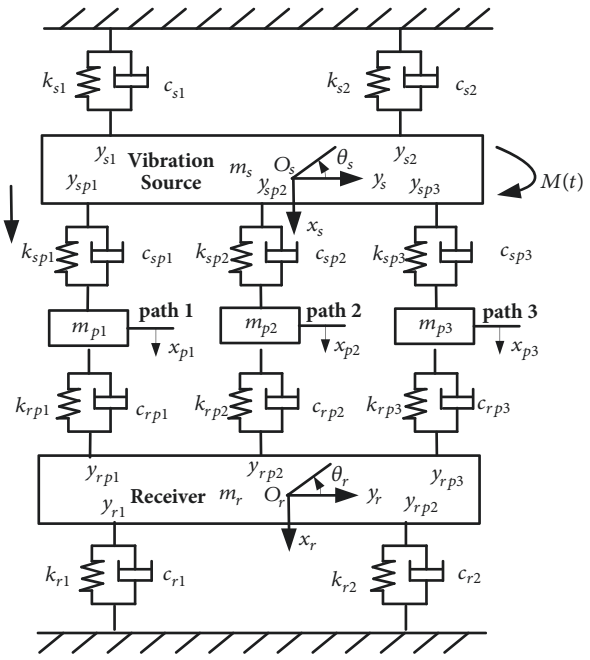

Figure 2: Vibration transfer path system model with linear motion and rotation.

equivalently equipped with a double-deck vibration isolator, which has higher vibration isolation performance. Owing to the asymmetry of its own structure or under the action of moment, the vibration system normally tends to rotate. Therefore, because of the occurrence of the swaying motions, not only physical parameters including path mass, stiffness, and damping, but also geometrical parameters such as position and shape would be reflected in the vibration transfer path system. The vibration source and receiver are regarded as rigid bodies, and the moments of inertia around the centroid can be denoted by I_s and I_r, respectively. The stiffness of the two fixed ends of the vibration source is represented by k_{s1} and k_{s2} with corresponding damping of c_{s1} and c_{s2}, respectively. Moreover, the stiffness of the two fixed ends of the receiver are denoted by k_{r1} and k_{r2} with corresponding damping of c_{r1} and c_{r2}. Relative to the centroid of the vibration source, the positions for the fixed ends of the vibration source are y_{s1} and y_{s2}, and the positions connecting the three paths with the vibration source are denoted by y_{sp1}, y_{sp2}, and y_{sp3}, respectively. Moreover, relative to the centroid of the receiver, the positions of the fixed ends of the receiver are y_{r1} and y_{r2}, and the positions connecting the three paths with the receiver are represented by y_{rp1}, y_{rp2}, and y_{rp3}. The vibration source is subjected to the vertical simple harmonic force excitation $F_0 \sin \omega t$. Owing to the distance between the force acting point and the centroid of the vibration source, the system simultaneously sustains the action by the moment $M_0 \sin \omega t$. The vertical and angular displacements for the centroid of the vibration source are denoted by x_s and θ_s; the vertical and angular displacements for the centroid of the receiver are x_r and θ_r; and the vertical displacements for the rigid masses of three paths are represented by x_{p1}, x_{p2}, and x_{p3}.

4. Path Contribution Analysis

The vibration transfer path system shown in Figure 1 can be depicted using two coordinates: $x_s(t)$ and $x_r(t)$. The vibration differential equation could be expressed as

$$\mathbf{M}_2 \ddot{\mathbf{x}}_2 + \mathbf{C}_2 \dot{\mathbf{x}}_2 + \mathbf{K}_2 \mathbf{x}_2 = \mathbf{F}_2(t) \tag{7}$$

where

$$\begin{aligned}
\mathbf{M}_2 &= \begin{bmatrix} m_s & 0 \\ 0 & m_r \end{bmatrix}; \\
\mathbf{C}_2 &= \begin{bmatrix} c_s + c_{p1} + c_{p2} + c_{p3} & -c_{p1} - c_{p2} - c_{p3} \\ -c_{p1} - c_{p2} - c_{p3} & c_r + c_{p1} + c_{p2} + c_{p3} \end{bmatrix}; \\
\mathbf{K}_2 &= \begin{bmatrix} k_s + k_{p1} + k_{p2} + k_{p3} & -k_{p1} - k_{p2} - k_{p3} \\ -k_{p1} - k_{p2} - k_{p3} & k_r + k_{p1} + k_{p2} + k_{p3} \end{bmatrix}; \\
\mathbf{x}_2 &= \begin{Bmatrix} x_s(t) \\ x_r(t) \end{Bmatrix}; \\
\mathbf{F}_2(t) &= \begin{Bmatrix} F_0 \sin \omega t \\ 0 \end{Bmatrix}
\end{aligned} \tag{8}$$

To analyze the complex frequency responses of the system, the complex vector $F_0 e^{i\omega t}$ was employed to denote excitations. Correspondingly, the steady-state responses of the vibration sources and receivers were, respectively, expressed as follows:

$$\begin{aligned}
x_s(t) &= X_s e^{i(\omega t - \varphi_s)}; \\
x_r(t) &= X_r e^{i(\omega t - \varphi_r)}
\end{aligned} \tag{9}$$

where X_s and X_r are real numbers that were determined by the excitation frequency ω and system parameters, while φ_s and φ_r represent phase angles for the responses of the vibration sources and receivers.

The following formulae, respectively, represent their velocity responses:

$$\begin{aligned}
\dot{x}_s(t) &= i\omega X_s e^{i(\omega t - \varphi_s)}; \\
\dot{x}_r(t) &= i\omega X_r e^{i(\omega t - \varphi_r)}
\end{aligned} \tag{10}$$

The characteristic determinant of the equation is written as

$$\det[Z(\omega)] = \det\left(-\omega^2 \mathbf{M}_2 + i\omega \mathbf{C}_2 + \mathbf{K}_2\right) \tag{11}$$

After substituting (7), (9), and (10) into (11), we obtained

$$\begin{aligned}\operatorname{Re}\{\det[Z(\omega)]\} &= \omega^4 m_s m_r \\ &\quad - \omega^2 \left[m_s \left(k_r + k_{p1} + k_{p2} + k_{p3} \right) \right. \\ &\quad + \left(c_s + c_{p1} + c_{p2} + c_{p3} \right) \left(c_r + c_{p1} + c_{p2} + c_{p3} \right) \\ &\quad \left. + m_r \left(k_s + k_{p1} + k_{p2} + k_{p3} \right) - \left(c_{p1} + c_{p2} + c_{p3} \right)^2 \right] \\ &\quad + \left(k_s + k_{p1} + k_{p2} + k_{p3} \right) \left(k_r + k_{p1} + k_{p2} + k_{p3} \right) \\ &\quad - \left(k_{p1} + k_{p2} + k_{p3} \right)^2 \operatorname{Im}\{\det[Z(\omega)]\} \\ &= -\omega^3 \left[m_s \left(c_r + c_{p1} + c_{p2} + c_{p3} \right) \right. \\ &\quad \left. + m_r \left(c_s + c_{p1} + c_{p2} + c_{p3} \right) \right] \\ &\quad + \omega \left[\left(c_s + c_{p1} + c_{p2} + c_{p3} \right) \left(k_r + k_{p1} + k_{p2} + k_{p3} \right) \right. \\ &\quad + \left(c_r + c_{p1} + c_{p2} + c_{p3} \right) \left(k_s + k_{p1} + k_{p2} + k_{p3} \right) \\ &\quad \left. - 2 \left(c_{p1} + c_{p2} + c_{p3} \right) \left(k_{p1} + k_{p2} + k_{p3} \right) \right]\end{aligned} \tag{12}$$

Accordingly, we derived

$$\begin{aligned}X_s(\omega)\, e^{-i\varphi_s} &= \frac{\left[-\omega^2 m_r + i\omega \left(c_r + c_{p1} + c_{p2} + c_{p3} \right) + \left(k_r + k_{p1} + k_{p2} + k_{p3} \right) \right] F_0}{\det[Z(\omega)]} \\ X_r(\omega)\, e^{-i\varphi_r} &= \frac{\left[i\omega \left(c_{p1} + c_{p2} + c_{p3} \right) + \left(k_{p1} + k_{p2} + k_{p3} \right) \right] F_0}{\det[Z(\omega)]}\end{aligned} \tag{13}$$

Hence, the amplitudes of steady-state responses could be expressed as

$$\begin{aligned}X_s &= \left| X_s(\omega)\, e^{-i\varphi_s} \right| = F_0 \sqrt{\frac{\left[-\omega^2 m_r + \left(k_r + k_{p1} + k_{p2} + k_{p3} \right) \right]^2 + \left[\omega \left(c_r + c_{p1} + c_{p2} + c_{p3} \right) \right]^2}{\left(\operatorname{Re}\{\det[Z(\omega)]\} \right)^2 + \left(\operatorname{Im}\{\det[Z(\omega)]\} \right)^2}} \\ X_r &= \left| X_r(\omega)\, e^{-i\varphi_r} \right| = F_0 \sqrt{\frac{\left(k_{p1} + k_{p2} + k_{p3} \right)^2 + \left[\omega \left(c_{p1} + c_{p2} + c_{p3} \right) \right]^2}{\left(\operatorname{Re}\{\det[Z(\omega)]\} \right)^2 + \left(\operatorname{Im}\{\det[Z(\omega)]\} \right)^2}}\end{aligned} \tag{14}$$

Obviously, the transfer force through the vibration transfer paths to the receiver is

$$\begin{aligned}F_{Tp_j} &= k_{pj} \left(x_r - x_s \right) + c_{pj} \left(\dot{x}_r - \dot{x}_s \right) \\ &= \left[k_{pj} \left(X_r - X_s \right) + i\omega c_{pj} \left(X_r - X_s \right) \right] e^{i(\omega t - \phi)} \\ &= \left(k_{pj} + i\omega c_{pj} \right) \left(X_r - X_s \right) e^{i(\omega t - \phi)} \quad (j = 1, 2, 3)\end{aligned} \tag{15}$$

The amplitude of the transfer force is

$$\left| F_{Tp_j} \right| = F_0 \sqrt{\frac{\left(k_{pj}^2 + \omega^2 c_{pj}^2 \right) \left[\omega^2 c_r^2 + \left(k_r - \omega^2 m_r \right)^2 \right]}{\left(\operatorname{Re}\{\det[Z(\omega)]\} \right)^2 + \left(\operatorname{Im}\{\det[Z(\omega)]\} \right)^2}} \quad (j = 1, 2, 3) \tag{16}$$

According to the definition, the TR of each path is

$$\begin{aligned}TR_j &= \left| \frac{F_{Tp_j}}{F_0} \right| \\ &= \sqrt{\frac{\left(k_{pj}^2 + \omega^2 c_{pj}^2 \right) \left[\omega^2 c_r^2 + \left(k_r - \omega^2 m_r \right)^2 \right]}{\left(\operatorname{Re}\{\det[Z(\omega)]\} \right)^2 + \left(\operatorname{Im}\{\det[Z(\omega)]\} \right)^2}} \quad (j = 1, 2, 3)\end{aligned} \tag{17}$$

By substituting the damping and stiffness parameters of each path in the formula, the TR of each transfer path can be calculated conveniently, and the contribution of each path to the vibration output of the receiver can be further evaluated.

For applying the other evaluation indicator of path contribution, that is, path IL, the path disconnect method can be used to analyze the vibration transfer path system. When path 1 was disconnected with path 2 and path 3 retained,

the various parameter matrixes for the vibration differential equation of the system are, respectively, written as follows:

$$\mathbf{C_{21}} = \begin{bmatrix} c_s + c_{p2} + c_{p3} & -c_{p2} - c_{p3} \\ -c_{p2} - c_{p3} & c_r + c_{p2} + c_{p3} \end{bmatrix};$$

$$\mathbf{K}_{21} = \begin{bmatrix} k_s + k_{p2} + k_{p3} & -k_{p2} - k_{p3} \\ -k_{p2} - k_{p3} & k_r + k_{p2} + k_{p3} \end{bmatrix}$$

$$\mathbf{M}_{21} = \begin{bmatrix} m_s & 0 \\ 0 & m_r \end{bmatrix}; \tag{18}$$

$$\mathbf{x_{21}} = \begin{Bmatrix} x_{s1} \\ x_{r1} \end{Bmatrix};$$

$$\mathbf{F_{21}}(t) = \begin{Bmatrix} F_0 e^{i\omega t} \\ 0 \end{Bmatrix}$$

The steady-state responses of the system can be written as

$$\begin{aligned} x_{s1}(t) &= X_{s1} e^{i(\omega t - \varphi_{s1})}; \\ x_{r1}(t) &= X_{r1} e^{i(\omega t - \varphi_{r1})} \end{aligned} \tag{19}$$

And the corresponding velocity responses are given by

$$\begin{aligned} \dot{x}_{s1}(t) &= i\omega X_{s1} e^{i(\omega t - \varphi_{s1})}; \\ \dot{x}_{r1}(t) &= i\omega X_{r1} e^{i(\omega t - \varphi_{r1})} \end{aligned} \tag{20}$$

where X_{s1} and X_{r1}, similarly, are the amplitudes expressed as real numbers, while φ_{s1} and φ_{r1} denote the initial phase angles for the responses of excitation source and system receiver.

The characteristic determinant of the system is

$$\det[Z1(\omega)] = \det\left(-\omega^2 \mathbf{M}_{21} + i\omega \mathbf{C}_{21} + \mathbf{K}_{21}\right) \tag{21}$$

The following expressions are derived by substituting the corresponding matrix:

$$\begin{aligned} \operatorname{Re}\{\det[Z1(\omega)]\} &= \omega^4 m_s m_r \\ &- \omega^2 \left[m_s \left(k_r + k_{p2} + k_{p3}\right) \right. \\ &+ \left(c_s + c_{p2} + c_{p3}\right)\left(c_r + c_{p2} + c_{p3}\right) \\ &\left. + m_r \left(k_s + k_{p2} + k_{p3}\right) - \left(c_{p2} + c_{p3}\right)^2 \right] + \left(k_s + k_{p2}\right. \\ &\left. + k_{p3}\right)\left(k_r + k_{p2} + k_{p3}\right) - \left(k_{p2} + k_{p3}\right)^2 \\ \cdot \operatorname{Im}\{\det[Z1(\omega)]\} &= -\omega^3 \left[m_s \left(c_r + c_{p2} + c_{p3}\right) \right. \\ &\left. + m_r \left(c_s + c_{p2} + c_{p3}\right) \right] \\ &+ \omega \left[\left(c_s + c_{p2} + c_{p3}\right)\left(k_r + k_{p2} + k_{p3}\right) \right. \\ &+ \left(c_r + c_{p2} + c_{p3}\right)\left(k_s + k_{p2} + k_{p3}\right) \\ &\left. - 2\left(c_{p2} + c_{p3}\right)\left(k_{p2} + k_{p3}\right) \right] \end{aligned} \tag{22}$$

Accordingly, we obtain

$$\begin{aligned} X_{s1}(\omega) e^{-i\varphi_{s1}} &= \frac{\left[-\omega^2 m_r + i\omega\left(c_r + c_{p2} + c_{p3}\right) + \left(k_r + k_{p2} + k_{p3}\right)\right] F_0}{\det[Z1(\omega)]} \\ X_{r1}(\omega) e^{-i\varphi_{r1}} &= \frac{\left[i\omega\left(c_{p2} + c_{p3}\right) + \left(k_{p2} + k_{p3}\right)\right] F_0}{\det[Z1(\omega)]} \end{aligned} \tag{23}$$

The amplitudes of the steady-state responses can be expressed as

$$\begin{aligned} X_{s1} &= \left| X_{s1}(\omega) e^{-i\varphi_{s1}} \right| \\ &= F_0 \sqrt{\frac{\left[-\omega^2 m_r + \left(k_r + k_{p2} + k_{p3}\right)\right]^2 + \left[\omega\left(c_r + c_{p2} + c_{p3}\right)\right]^2}{\left(\operatorname{Re}\{\det[Z1(\omega)]\}\right)^2 + \left(\operatorname{Im}\{\det[Z1(\omega)]\}\right)^2}} \\ X_{r1} &= \left| X_{r1}(\omega) e^{-i\varphi_{r1}} \right| \\ &= F_0 \sqrt{\frac{\left(k_{p2} + k_{p3}\right)^2 + \left[\omega\left(c_{p2} + c_{p3}\right)\right]^2}{\left(\operatorname{Re}\{\det[Z1(\omega)]\}\right)^2 + \left(\operatorname{Im}\{\det[Z1(\omega)]\}\right)^2}} \end{aligned} \tag{24}$$

According to (4), the velocity IL of path 1 is written as

$$\begin{aligned} IL_{v1} &= 20 \lg \left| \frac{\dot{x}_{r1}(t)}{\dot{x}_r(t)} \right| = 20 \lg \left| \frac{X_{r1} e^{-i\varphi_{r1}}}{X_r e^{-i\varphi_r}} \right| = 10 \\ &\cdot \lg \left\{ \frac{\left(k_{p2} + k_{p3}\right)^2 + \left[\omega\left(c_{p2} + c_{p3}\right)\right]^2}{\left(k_{p1} + k_{p2} + k_{p3}\right)^2 + \left[\omega\left(c_{p1} + c_{p2} + c_{p3}\right)\right]^2} \right. \\ &\left. \cdot \frac{\left(\operatorname{Re}\{\det[Z(\omega)]\}\right)^2 + \left(\operatorname{Im}\{\det[Z(\omega)]\}\right)^2}{\left(\operatorname{Re}\{\det[Z_1(\omega)]\}\right)^2 + \left(\operatorname{Im}\{\det[Z_1(\omega)]\}\right)^2} \right\} \end{aligned} \tag{25}$$

Similarly, when path 2 and path 3 are disconnected severally, the corresponding velocity ILs are, respectively, expressed as follows:

$$\begin{aligned} IL_{v2} &= 20 \lg \left| \frac{\dot{x}_{r2}(t)}{\dot{x}_r(t)} \right| = 20 \lg \left| \frac{X_{r2} e^{-i\varphi_{r1}}}{X_r e^{-i\varphi_r}} \right| = 10 \\ &\cdot \lg \left\{ \frac{\left(k_{p1} + k_{p3}\right)^2 + \left[\omega\left(c_{p1} + c_{p3}\right)\right]^2}{\left(k_{p1} + k_{p2} + k_{p3}\right)^2 + \left[\omega\left(c_{p1} + c_{p2} + c_{p3}\right)\right]^2} \right. \\ &\left. \cdot \frac{\left(\operatorname{Re}\{\det[Z(\omega)]\}\right)^2 + \left(\operatorname{Im}\{\det[Z(\omega)]\}\right)^2}{\left(\operatorname{Re}\{\det[Z_2(\omega)]\}\right)^2 + \left(\operatorname{Im}\{\det[Z_2(\omega)]\}\right)^2} \right\} \end{aligned} \tag{26}$$

$$\begin{aligned} IL_{v3} &= 20 \lg \left| \frac{\dot{x}_{r3}(t)}{\dot{x}_r(t)} \right| = 20 \lg \left| \frac{X_{r3} e^{-i\varphi_{r1}}}{X_r e^{-i\varphi_r}} \right| = 10 \\ &\cdot \lg \left\{ \frac{\left(k_{p1} + k_{p2}\right)^2 + \left[\omega\left(c_{p1} + c_{p2}\right)\right]^2}{\left(k_{p1} + k_{p2} + k_{p3}\right)^2 + \left[\omega\left(c_{p1} + c_{p2} + c_{p3}\right)\right]^2} \right. \\ &\left. \cdot \frac{\left(\operatorname{Re}\{\det[Z(\omega)]\}\right)^2 + \left(\operatorname{Im}\{\det[Z(\omega)]\}\right)^2}{\left(\operatorname{Re}\{\det[Z_3(\omega)]\}\right)^2 + \left(\operatorname{Im}\{\det[Z_3(\omega)]\}\right)^2} \right\} \end{aligned} \tag{27}$$

The velocity IL can analyze the influence of every path to the velocity response of the receiver and evaluate the path contribution to the system vibration output.

Both evaluation indicators can be used to analyze the path contributions to the system vibration response when path stiffness parameters and path damping parameters are matched differently. For the vibration transfer path systems without considering the path mass parameters, the above theoretical analysis and calculation formula can greatly simplify the optimization design process for the mechanical systems.

For the system shown in Figure 2, the vibration differential equation is derived using Lagrange's equation considering the microvibrations of the system.

$$\mathbf{M}_7\ddot{\mathbf{x}}_7 + \mathbf{C}_7\dot{\mathbf{x}}_7 + \mathbf{K}_7\mathbf{x}_7 = \mathbf{F}_7(t) \tag{28}$$

The matrixes in the differential equation are shown in formulae (A.1)-(A.5) in Appendix.

When analyzing the complex frequency responses of the system, complex vectors $F_0e^{i\omega t}$ and $M_0e^{i\omega t}$ are employed to denote excitations. Thereby, the steady-state response of the system can be expressed as

$$\mathbf{X}_7(t) = e^{i\omega t}\left\{X_s e^{i\varphi_{xs}} \quad \theta_s e^{i\varphi_{\theta s}} \quad X_{p1}e^{i\varphi_{p1}} \quad X_{p2}e^{i\varphi_{p2}} \quad X_{p3}e^{i\varphi_{p3}} \quad X_r e^{i\varphi_{xr}} \quad \theta_r e^{i\varphi_{\theta r}}\right\}^T \tag{29}$$

where X_s, θ_s, X_{p1}, X_{p2}, X_{p3}, X_r, and θ_r are real numbers that were determined by the excitation frequency ω and system parameters, while φ_{xs}, $\varphi_{\theta s}$, φ_{p1}, φ_{p2}, φ_{p3}, φ_{xr}, and $\varphi_{\theta r}$ denote the phase angles of the system vibration source, path 1, path 2, path 3, and the receiver, respectively.

Substituting (29) into (28),

$$\left(-\omega^2\mathbf{M}_7 + i\omega\mathbf{C}_7 + \mathbf{K}_7\right)\mathbf{X}_7 = \mathbf{F}_7 \tag{30}$$

where

$$\begin{aligned}\mathbf{X}_7 &= \left\{X_s e^{i\eta_{xs}} \quad \theta_s e^{i\eta_{\theta s}} \quad X_{p1}e^{i\eta_{p1}} \quad X_{p2}e^{i\eta_{p2}} \quad X_{p3}e^{i\eta_{p3}} \quad X_r e^{i\eta_{xr}} \quad \theta_r e^{i\eta_{\theta r}}\right\}^T;\\ \mathbf{F}_7 &= \left(F_0 \quad M_0 \quad 0 \quad 0 \quad 0 \quad 0 \quad 0\right)\end{aligned} \tag{31}$$

The characteristic of the vibration transfer path system lays in that the paths are subjected to the effect of mass parameters. In addition, the system is characterized by coupled rectilinear and swaying motions. The path transfer force of each path is

$$\begin{aligned}F_{Tp_j} &= k_{rpj}\left(x_r - x_{pj} - y_{rpj}\theta_r\right) + c_{rpj}\left(\dot{x}_r - \dot{x}_{pj}\right.\\ &\left. - y_{rpj}\dot{\theta}_r\right) = \left[k_{rpj}\left(X_r e^{i\eta_{xr}} - X_{pj}e^{i\eta_{pj}} - y_{rpj}\theta_r e^{i\eta_{\theta r}}\right)\right.\\ &\left. + i\omega c_{rpj}\left(X_r e^{i\eta_{xr}} - X_{pj}e^{i\eta_{pj}} - y_{rpj}\theta_r e^{i\eta_{\theta r}}\right)\right]e^{i\omega t}\\ &= \left[\left(k_{rpj} + i\omega c_{rpj}\right)\right.\\ &\left.\cdot\left(X_r e^{i\eta_{xr}} - X_{pj}e^{i\eta_{pj}} - y_{rpj}\theta_r e^{i\eta_{\theta r}}\right)\right]e^{i\omega t}\\ &\qquad\qquad (j = 1, 2, 3)\end{aligned} \tag{32}$$

The corresponding path TR is

$$\begin{aligned}TR_j &= \left|\frac{F_{Tp_j}}{F_0}\right|\\ &= \left|\frac{\left(k_{rpj} + i\omega c_{rpj}\right)\left(X_r e^{i\eta_{xr}} - X_{pj}e^{i\eta_{pj}} - y_{rpj}\theta_r e^{i\eta_{\theta r}}\right)}{F_0}\right|\\ &\qquad\qquad (j = 1, 2, 3)\end{aligned} \tag{33}$$

The receiver response values in the frequency domain can be obtained by matrix computation. Thus, the path TR of each path can be calculated with path parameters.

When path 1 is disconnected with path 2 and path 3 retained. This system has the same form of vibration differential equation with the original system, and the matrixes in the equation are shown in the formulae (A.6)-(A.10) in Appendix.

The steady-state response is

$$\mathbf{X}_{71}(t) = e^{i\omega t}\left\{X_{1s}e^{i\eta_{1xs}} \quad \theta_{1s}e^{i\eta_{1\theta s}} \quad X_{1p2}e^{i\eta_{1p2}} \quad X_{1p3}e^{i\eta_{1p3}} \quad X_{1r}e^{i\eta_{1xr}} \quad \theta_{1r}e^{i\eta_{1\theta r}}\right\}^T \tag{34}$$

where X_{1s}, θ_{1s}, X_{1p2}, X_{1p3}, X_{1r}, and θ_{1r} are real numbers that are determined by the excitation frequency ω and system parameters, while η_{1xs}, $\eta_{1\theta s}$, η_{1p2}, η_{1p3}, η_{1xr}, and $\eta_{1\theta r}$ represent the phase angles for the responses of the linear displacement of the system vibration source, angular displacement of the vibration source, path 2, path 3, linear displacement of the receivers, and angular displacement of the receivers, respectively.

The corresponding velocity response is given by

$$\dot{\mathbf{X}}_{71}(t) = i\omega e^{i\omega t}\left\{X_{1s}e^{i\eta_{1xs}} \;\; \theta_{1s}e^{i\eta_{1\theta s}} \;\; X_{1p2}e^{i\eta_{1p2}} \;\; X_{1p3}e^{i\eta_{1p3}} \;\; X_{1r}e^{i\eta_{1xr}} \;\; \theta_{1r}e^{i\eta_{1\theta r}}\right\}^T \tag{35}$$

Thus, the system vibration equation can be written as

$$\left(-\omega^2\mathbf{M}_{71} + i\omega\mathbf{C}_{71} + \mathbf{K}_{71}\right)\mathbf{X}_{71} = \mathbf{F}_{71} \tag{36}$$

where

$$\begin{aligned}&\mathbf{X}_{71}\\ &= \left\{X_{1s}e^{i\eta_{1xs}} \;\; \theta_{1s}e^{i\eta_{1\theta s}} \;\; X_{1p2}e^{i\eta_{1p2}} \;\; X_{1p3}e^{i\eta_{1p3}} \;\; X_{1r}e^{i\eta_{1xr}} \;\; \theta_{1r}e^{i\eta_{1\theta r}}\right\}^T;\\ &\mathbf{F}_{71} = \{F_0 \;\; M_0 \;\; 0 \;\; 0 \;\; 0 \;\; 0\}\end{aligned} \tag{37}$$

It is known that the receiver energy can be calculated as follows:

$$\begin{aligned}E_{r1}(\omega) &= \frac{1}{2}m_r\dot{x}_{1r}^2 + \frac{1}{2}I_r\dot{\theta}_{1r}^2\\ &= -\frac{1}{2}\omega^2 e^{2i\omega t}\left[m_r\left(X_{1r}e^{i\eta_{1xr}}\right)^2 + I_r\left(\theta_{1r}e^{i\eta_{1\theta r}}\right)^2\right]\end{aligned} \tag{38}$$

The energy IL of path 1 is

$$\begin{aligned}IL_{E1} &= 10\lg\left|\frac{\dot{E}_{1r}(t)}{\dot{E}_r(t)}\right|\\ &= 10\lg\left|\frac{m_r\left(X_{1r}e^{i\eta_{1xr}}\right)^2 + I_r\left(\theta_{1r}e^{i\eta_{1\theta r}}\right)^2}{m_r\left(X_re^{i\eta_{xr}}\right)^2 + I_r\left(\theta_re^{i\eta_{\theta r}}\right)^2}\right|\end{aligned} \tag{39}$$

Similarly, when path 2 is disconnected, the matrixes in the equation are shown in the formulae (A.11)-(A.15) in Appendix. When path 3 is disconnected, the matrixes in the equation are shown in the formulae (A.16)-(A.20) in Appendix. The corresponding energy ILs are, respectively, expressed as follows:

$$\begin{aligned}IL_{E2} &= 10\lg\left|\frac{\dot{E}_{r2}(t)}{\dot{E}_r(t)}\right|\\ &= 10\lg\left|\frac{m_r\left(X_{2r}e^{i\eta_{2xr}}\right)^2 + I_r\left(\theta_{2r}e^{i\eta_{2\theta r}}\right)^2}{m_r\left(X_re^{i\eta_{xr}}\right)^2 + I_r\left(\theta_re^{i\eta_{\theta r}}\right)^2}\right|\end{aligned} \tag{40}$$

$$\begin{aligned}IL_{E3} &= 10\lg\left|\frac{\dot{E}_{r3}(t)}{\dot{E}_r(t)}\right|\\ &= 10\lg\left|\frac{m_r\left(X_{3r}e^{i\eta_{3xr}}\right)^2 + I_r\left(\theta_{3r}e^{i\eta_{3\theta r}}\right)^2}{m_r\left(X_re^{i\eta_{xr}}\right)^2 + I_r\left(\theta_re^{i\eta_{\theta r}}\right)^2}\right|\end{aligned} \tag{41}$$

From the theoretical analysis, it can be seen that the path mass parameters and the path position parameters are important for the path contributions. The model shown in Figure 2 can be used to analyze the complex vibration transfer path systems. On the basis of finding the transfer path with the greatest contribution to the system response, the physical and geometric parameters of the path are optimized simultaneously to achieve the optimal matching of various parameters.

5. Numerical Example

Example 1. For the vibration transfer path system illustrated in Figure 1, we design the system parameters listed in Table 1.

The natural frequencies of the vibration system are calculated as follows:

$$\begin{aligned}\omega_1 &= 12.3725\,(\text{rad/s}),\\ \omega_2 &= 67.2220/\,(\text{rad/s})\end{aligned} \tag{42}$$

The characteristic curves of path TR and velocity IL versus excitation frequencies can be obtained according to the previous theoretical analysis, as illustrated in Figures 3 and 4.

As shown in Figure 3, the path transfer ratio is very high at two natural frequencies. In the whole resonance frequency range, the transfer ratios of the three transfer paths are clearly sorted.

$$TR_1 > TR_3 > TR_2 \tag{43}$$

For the insertion loss, the positive value indicates that the response value of the system receiver decreases after the path is connected and the negative one shows the increase of the vibration response value after the path is connected. According to the definition, the purpose of insertion loss is to evaluate the influence degree to the receiver response after joining the system. Therefore, the positive and negative of the insertion loss can be ignored, and only the absolute value is considered. As shown in Figure 4, the IL for each path exhibits two extreme values in the entire resonance frequency range. Moreover, the first extreme value of each characteristic curves occurred, respectively, at the location of the second-order natural frequency of various disconnect systems. The second one occurs at the location of the second-order natural frequency of the system prior to path disconnect, wherein path 1 exhibits a larger IL compared to that of path 3, and the IL of path 3 is greater than that of path 2. Therefore, the second-order natural frequency of the vibration system is

Table 1: The parameters of the system shown in Figure 1.

Excitation	$F_0 = 10\text{N}$
Vibration source	$m_s = 0.7724\text{kg}$, $c_s = 0.5\text{N·s/m}$, $k_s = 100\text{N/m}$
Transfer path	$m_r = 1.0556\text{kg}$, $c_r = 1.0\text{N·s/m}$, $k_r = 180\text{N/m}$
Receiver	$c_{p1} = 1.0\text{N·s/m}$, $c_{p2} = 1.5\text{N·s/m}$, $c_{p3} = 0.5\text{N·s/m}$, $k_{p1} = 900\text{N/m}$, $k_{p2} = 450\text{N/m}$, $k_{p3} = 600\text{N/m}$.

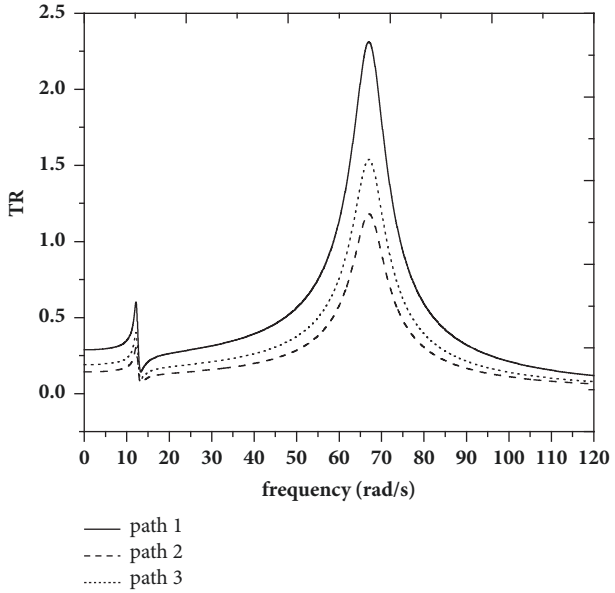

Figure 3: The curve of path TR with regard to excitation frequency.

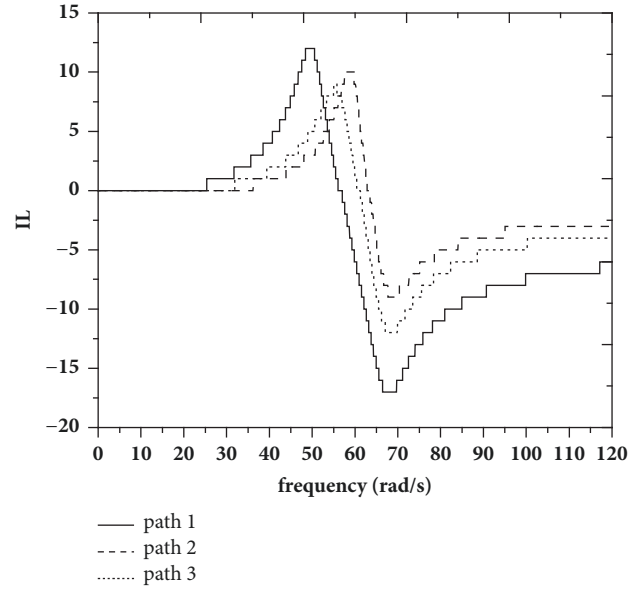

Figure 4: The curve of the path IL with respect to the excitation frequency.

the most dangerous frequency point and the vibration source should try to avoid working near this frequency point.

In order to compare the contributions of various paths in the process of vibration transfer more easily and quantitatively, the average IL within a certain frequency range is regarded as an effective evaluation indicator, expressed as

$$IL_{vj,Ave} = \frac{1}{N_b - N_a + 1} \sum_{\omega=N_a}^{N_b} \left| 20 \log_{10} \left| \frac{\dot{x}_{rj}}{\dot{x}_r} \right| \right| \quad (j = 1, 2, 3) \tag{44}$$

where N_a is the counting point for the starting frequency of the average values, while N_b denotes that of the ending frequency of average values. Generally, to avoid the numerical divergence at zero frequency, a value of 1 may be assigned to the counting point for the starting frequency when calculating the average value. The value for the counting point of the ending frequency can be determined as approximately 1.5 times of the highest-order natural frequency. Here the 10000-th counting point is selected.

Based on the above formula, the average of path IL can be calculated and the results are as follows:

$$\begin{aligned} IL_{v1,Ave} &= 6.7276; \\ IL_{v2,Ave} &= 3.6796; \\ IL_{v3,Ave} &= 4.6742 \\ IL_{v1,Ave} &> IL_{v3,Ave} > IL_{v2,Ave} \end{aligned} \tag{45}$$

Two methods are applied to analyze the path contributions of the vibration transfer path system, and the same sort results are obtained: Path 1 exhibits a larger contribution for the vibration transfer to the receiver, followed by the contribution of path 3, and that of path 2 is comparatively smaller. Hence, path 1 remains the most important transfer path.

Example 2. Consider the model of the vibration transfer path system having coupled rectilinear and swaying motions as shown in Figure 2. The system parameters are listed in Table 2.

Table 2: The parameters of the system shown in Figure 2.

Excitation	F_0 =10N, y_f = 0.02m (excitation location)
Vibration source	m_s = 0.7724kg, c_{s1} = 0.5N·s/m, c_{s2} = 0.5N·s/m, k_{s1} = 100N/m, k_{s2} = 100N/m, I_{sz} = 2.5799 × 10^{-3}kg·m^2 (moment of inertia), y_{s1} = -0.10m, y_{s2} = 0.10m.
Transfer path	m_{p1} = 0.9kg, m_{p2} = 0.5kg, m_{p3} = 0.6kg, c_{sp1} = c_{rp1} = 1.0N·s/m, c_{sp2} = c_{rp2} = 1.5N·s/m, c_{sp3} = c_{rp3} = 0.5N·s/m, k_{sp1} = k_{rp1} = 900N/m, k_{sp2} = k_{rp2} = 450N/m, k_{sp3} = k_{rp3} = 600N/m, y_{sp1} = -0.09m, y_{rp1} = -0.10m, y_{sp2} = -0.03m, y_{rp2} = -0.04m, y_{sp3} = 0.10m, y_{rp3} = 0.09m.
Receiver	m_r = 1.0556kg, c_{r1} = 1.0N·s/m c_{r2} = 1.0N·s/m, k_{r1} = 180N/m, k_{r2} = 180N/m, I_{rz} = 7.8722 × 10^{-3}kg·m^2 (moment of inertia), y_{r1} = -0.15m, y_{r2} = 0.15m.

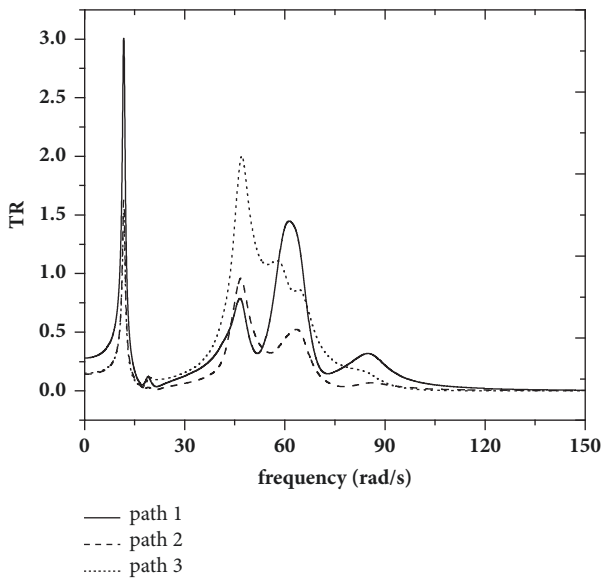

Figure 5: Characteristic curve of the path TR with respect to excitation frequency.

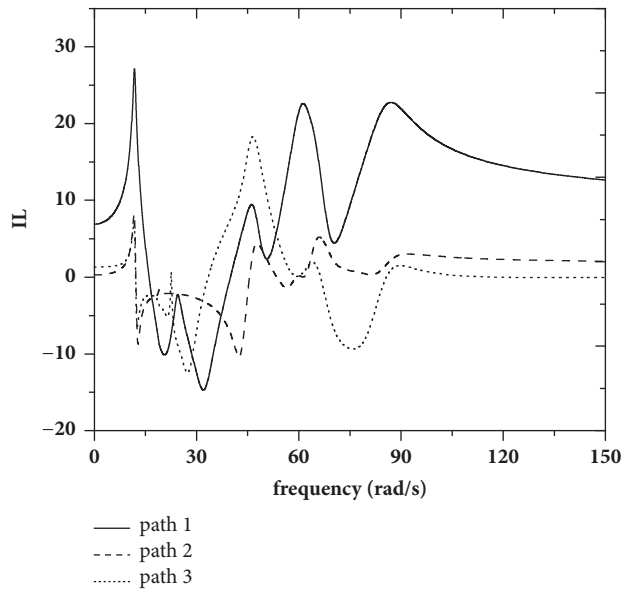

Figure 6: Characteristic curve of the path IL with respect to excitation frequency.

The natural frequencies of the system are as follows:

$$\begin{aligned} \omega_1 &= 11.7566, \\ \omega_2 &= 19.0825, \\ \omega_3 &= 42.8390, \\ \omega_4 &= 46.8275, \\ \omega_5 &= 59.3125, \\ \omega_6 &= 65.1858, \\ \text{and } \omega_7 &= 85.8403 \end{aligned} \tag{46}$$

The calculation results of path TR and energy IL are shown in Figures 5 and 6.

From Figure 5, we can see that the curves have peak values at each natural frequency point. In addition, in the frequency range before the fifth order natural frequency, the transfer ratio of path 3 is the largest. Path 3 is the most important transfer path. In the frequency range between the fifth order natural frequency and the seventh order natural frequency, the transfer ratio of path 1 is the highest and path 1 is the most important transfer path. The transfer ratio of path 2 in the whole natural frequency range is the lowest.

In order to quantitatively evaluate the transfer ratio of each path in the whole resonance frequency range, the averages of path transfer ratios are calculated. The selection of frequency range and count point is consistent with that of path IL calculation. The results are as follows:

$$\begin{aligned} TR_{1,Ave} &= 0.1884, \\ TR_{2,Ave} &= 0.0797, \\ TR_{3,Ave} &= 0.1636 \\ TR_{1,Ave} &> TR_{3,Ave} > TR_{2,Ave} \end{aligned} \tag{47}$$

Comparing Figure 6 with Figure 5, we can see that the trend of the two sets of curves keeps consistent at each frequency point and the orders of path contribution are also the same.

The averages of the path ILs are as follows:

$$\begin{aligned} IL_{E1,Ave} &= 12.6243, \\ IL_{E2,Ave} &= 8.4231, \\ IL_{E3,Ave} &= 9.3825 \\ IL_{E1,Ave} &> IL_{E3,Ave} > IL_{E2,Ave} \end{aligned} \tag{48}$$

From the averages of path TRs and path ILs, the order of path contributions in the whole resonance frequency range is as follows: Path 1 exhibits the largest contribution to the vibration transfer, followed by path 3, and that of path 2 is comparatively the smallest.

6. Conclusions

Two kinds of vibration transfer path systems are developed in this work. One kind only has translational motions. The other kind includes not only the translational motions but also the rotational motions because of the change in the vibration source characteristics. Thereby, the physical and geometric parameters have the mixed influence on the transfer path characteristics.

With respect to the multiple transfer paths in the systems, the contribution rank is the key problem for the system dynamic design. The path TR and path IL are proved to be effective evaluation indicators. According to the formulae derived in this work, we obtain the characteristic curves of the path TR and path IL varying with the frequency in the entire resonance frequency range. Based on the analysis results, the most important transfer path can be found for the actual working frequencies. In order to get the quantitative rank of path contributions, the corresponding averages are given furthermore, which makes the path comparison more convenient and easier

The proposed analytical method can be used at the design stage rather than for diagnostic purpose. With the aid of the ranking results, designers can rapidly and accurately identify the critical transfer path and modify the corresponding path parameters to satisfy the requirements of vibrations and noises.

Appendix

Formulae

$$\mathbf{M}_7 = \operatorname{diag}\left(m_s \;\; I_s \;\; m_{p1} \;\; m_{p2} \;\; m_{p3} \;\; m_r \;\; I_r\right) \tag{A.1}$$

$$\mathbf{C}_7 = \begin{bmatrix} \sum c_{sn} & -\sum c_{sn}y_{sn} & -c_{sp1} & -c_{sp2} & -c_{sp3} & 0 & 0 \\ -\sum c_{sn}y_{sn} & \sum c_{sn}y^2{}_{sn} & c_{sp1}y_{sp1} & c_{sp2}y_{sp2} & c_{sp3}y_{sp3} & 0 & 0 \\ -c_{sp1} & c_{sp1}y_{sp1} & c_{sp1}+c_{rp1} & 0 & 0 & -c_{rp1} & c_{rp1}y_{rp1} \\ -c_{sp2} & c_{sp2}y_{sp2} & 0 & c_{sp2}+c_{rp2} & 0 & -c_{rp2} & c_{rp2}y_{rp2} \\ -c_{sp3} & c_{sp3}y_{sp3} & 0 & 0 & c_{sp3}+c_{rp3} & -c_{rp3} & c_{rp3}y_{rp3} \\ 0 & 0 & -c_{rp1} & -c_{rp2} & -c_{rp3} & \sum c_{rn} & -\sum c_{rn}y_{rn} \\ 0 & 0 & c_{rp1}y_{rp1} & c_{rp2}y_{rp2} & c_{rp3}y_{rp3} & -\sum c_{rn}y_{rn} & \sum c_{rn}y^2{}_{rn} \end{bmatrix} \tag{A.2}$$

$$\mathbf{K}_7 = \begin{bmatrix} \sum k_{sn} & -\sum k_{sn}y_{sn} & -k_{sp1} & -k_{sp2} & -k_{sp3} & 0 & 0 \\ -\sum k_{sn}y_{sn} & \sum k_{sn}y^2{}_{sn} & k_{sp1}y_{sp1} & k_{sp2}y_{sp2} & k_{sp3}y_{sp3} & 0 & 0 \\ -k_{sp1} & k_{sp1}y_{sp1} & k_{sp1}+k_{rp1} & 0 & 0 & -k_{rp1} & k_{rp1}y_{rp1} \\ -k_{sp2} & k_{sp2}y_{sp2} & 0 & k_{sp2}+k_{rp2} & 0 & -k_{rp2} & k_{rp2}y_{rp2} \\ -k_{sp3} & k_{sp3}y_{sp3} & 0 & 0 & k_{sp3}+k_{rp3} & -k_{rp3} & k_{rp3}y_{rp3} \\ 0 & 0 & -k_{rp1} & -k_{rp2} & -k_{rp3} & \sum k_{rn} & -\sum k_{rn}y_{rn} \\ 0 & 0 & k_{rp1}y_{rp1} & k_{rp2}y_{rp2} & k_{rp3}y_{rp3} & -\sum k_{rn}y_{rn} & \sum k_{rn}y^2{}_{rn} \end{bmatrix} \tag{A.3}$$

where $n = 1, 2, p1, p2, p3$.

$$\mathbf{F}_7(t) = \{F_0 \sin(\omega t) \;\; M_0 \sin(\omega t) \;\; 0 \;\; 0 \;\; 0 \;\; 0 \;\; 0\} \tag{A.4}$$

$$\mathbf{x}_7(t) = \{x_s \;\; \theta_s \;\; x_{p1} \;\; x_{p2} \;\; x_{p3} \;\; x_r \;\; \theta_r\} \tag{A.5}$$

$$\mathbf{M}_{71} = \operatorname{diag}\left(m_s \;\; I_s \;\; m_{p2} \;\; m_{p3} \;\; m_r \;\; I_r\right) \tag{A.6}$$

$$\mathbf{C}_{71} = \begin{bmatrix} \sum c_{sn} & -\sum c_{sn}y_{sn} & -c_{sp2} & -c_{sp3} & 0 & 0 \\ -\sum c_{sn}y_{sn} & \sum c_{sn}y^2{}_{sn} & c_{sp2}y_{sp2} & c_{sp3}y_{sp3} & 0 & 0 \\ -c_{sp2} & c_{sp2}y_{sp2} & c_{sp2}+c_{rp2} & 0 & -c_{rp2} & c_{rp2}y_{rp2} \\ -c_{sp3} & c_{sp3}y_{sp3} & 0 & c_{sp3}+c_{rp3} & -c_{rp3} & c_{rp3}y_{rp3} \\ 0 & 0 & -c_{rp2} & -c_{rp3} & \sum c_{rn} & -\sum c_{rn}y_{rn} \\ 0 & 0 & c_{rp2}y_{rp2} & c_{rp3}y_{rp3} & -\sum c_{rn}y_{rn} & \sum c_{rn}y^2{}_{rn} \end{bmatrix} \tag{A.7}$$

$$\mathbf{K}_{71} = \begin{bmatrix} \sum k_{sn} & -\sum k_{sn}y_{sn} & -k_{sp2} & -k_{sp3} & 0 & 0 \\ -\sum k_{sn}y_{sn} & \sum k_{sn}y^2{}_{sn} & k_{sp2}y_{sp2} & k_{sp3}y_{sp3} & 0 & 0 \\ -k_{sp2} & k_{sp2}y_{sp2} & k_{sp2}+k_{rp2} & 0 & -k_{rp2} & k_{rp2}y_{rp2} \\ -k_{sp3} & k_{sp3}y_{sp3} & 0 & k_{sp3}+k_{rp3} & -k_{rp3} & k_{rp3}y_{rp3} \\ 0 & 0 & -k_{rp2} & -k_{rp3} & \sum k_{rn} & -\sum k_{rn}y_{rn} \\ 0 & 0 & k_{rp2}y_{rp2} & k_{rp3}y_{rp3} & -\sum k_{rn}y_{rn} & \sum k_{rn}y^2{}_{rn} \end{bmatrix} \tag{A.8}$$

where $n = 1, 2, p2, p3$.

$$\mathbf{F}_{71}(t) = \{F_0 \sin(\omega t) \quad M_0 \sin(\omega t) \quad 0 \quad 0 \quad 0 \quad 0\} \tag{A.9}$$

$$\mathbf{X}_{71}(t) = \{x_{1s} \quad \theta_{1s} \quad x_{1p2} \quad x_{1p3} \quad x_{1r} \quad \theta_{1r}\} \tag{A.10}$$

$$\mathbf{M}_{72} = \operatorname{diag}(m_s \quad I_s \quad m_{p1} \quad m_{p3} \quad m_r \quad I_r) \tag{A.11}$$

$$\mathbf{C}_{72} = \begin{bmatrix} \sum c_{sn} & -\sum c_{sn}y_{sn} & -c_{sp1} & -c_{sp3} & 0 & 0 \\ -\sum c_{sn}y_{sn} & \sum c_{sn}y^2{}_{sn} & c_{sp1}y_{sp1} & c_{sp3}y_{sp3} & 0 & 0 \\ -c_{sp1} & c_{sp1}y_{sp1} & c_{sp1}+c_{rp1} & 0 & -c_{rp1} & c_{rp1}y_{rp1} \\ -c_{sp3} & c_{sp3}y_{sp3} & 0 & c_{sp3}+c_{rp3} & -c_{rp3} & c_{rp3}y_{rp3} \\ 0 & 0 & -c_{rp1} & -c_{rp3} & \sum c_{rn} & -\sum c_{rn}y_{rn} \\ 0 & 0 & c_{rp1}y_{rp1} & c_{rp3}y_{rp3} & -\sum c_{rn}y_{rn} & \sum c_{rn}y^2{}_{rn} \end{bmatrix} \tag{A.12}$$

$$\mathbf{K}_{72} = \begin{bmatrix} \sum k_{sn} & -\sum k_{sn}y_{sn} & -k_{sp1} & -k_{sp3} & 0 & 0 \\ -\sum k_{sn}y_{sn} & \sum k_{sn}y^2{}_{sn} & k_{sp1}y_{sp1} & k_{sp3}y_{sp3} & 0 & 0 \\ -k_{sp1} & k_{sp1}y_{sp1} & k_{sp1}+k_{rp1} & 0 & -k_{rp1} & k_{rp1}y_{rp1} \\ -k_{sp3} & k_{sp3}y_{sp3} & 0 & k_{sp3}+k_{rp3} & -k_{rp3} & k_{rp3}y_{rp3} \\ 0 & 0 & -k_{rp1} & -k_{rp3} & \sum k_{rn} & -\sum k_{rn}y_{rn} \\ 0 & 0 & k_{rp1}y_{rp1} & k_{rp3}y_{rp3} & -\sum k_{rn}y_{rn} & \sum k_{rn}y^2{}_{rn} \end{bmatrix} \tag{A.13}$$

where $n = 1, 2, p1, p3$.

$$\mathbf{F}_{72}(t) = \{F_0 \sin(\omega t) \quad M_0 \sin(\omega t) \quad 0 \quad 0 \quad 0 \quad 0\} \tag{A.14}$$

$$\mathbf{X}_{72}(t) = \{x_{2s} \quad \theta_{2s} \quad x_{2p1} \quad x_{2p3} \quad x_{2r} \quad \theta_{2r}\} \tag{A.15}$$

$$\mathbf{M}_{73} = \operatorname{diag}(m_s \quad I_s \quad m_{p1} \quad m_{p2} \quad m_r \quad I_r) \tag{A.16}$$

$$\mathbf{C}_{73} = \begin{bmatrix} \sum c_{sn} & -\sum c_{sn}y_{sn} & -c_{sp1} & -c_{sp2} & 0 & 0 \\ -\sum c_{sn}y_{sn} & \sum c_{sn}y^2{}_{sn} & c_{sp1}y_{sp1} & c_{sp2}y_{sp2} & 0 & 0 \\ -c_{sp1} & c_{sp1}y_{sp1} & c_{sp1}+c_{rp1} & 0 & -c_{rp1} & c_{rp1}y_{rp1} \\ -c_{sp2} & c_{sp2}y_{sp2} & 0 & c_{sp2}+c_{rp2} & -c_{rp2} & c_{rp2}y_{rp2} \\ 0 & 0 & -c_{rp1} & -c_{rp2} & \sum c_{rn} & -\sum c_{rn}y_{rn} \\ 0 & 0 & c_{rp1}y_{rp1} & c_{rp2}y_{rp2} & -\sum c_{rn}y_{rn} & \sum c_{rn}y^2{}_{rn} \end{bmatrix} \quad \text{(A.17)}$$

$$\mathbf{K}_{73} = \begin{bmatrix} \sum k_{sn} & -\sum k_{sn}y_{sn} & -k_{sp1} & -k_{sp2} & 0 & 0 \\ -\sum k_{sn}y_{sn} & \sum k_{sn}y^2{}_{sn} & k_{sp1}y_{sp1} & k_{sp2}y_{sp2} & 0 & 0 \\ -k_{sp1} & k_{sp1}y_{sp1} & k_{sp1}+k_{rp1} & 0 & -k_{rp1} & k_{rp1}y_{rp1} \\ -k_{sp2} & k_{sp2}y_{sp2} & 0 & k_{sp2}+k_{rp2} & -k_{rp2} & k_{rp2}y_{rp2} \\ 0 & 0 & -k_{rp1} & -k_{rp2} & \sum k_{rn} & -\sum k_{rn}y_{rn} \\ 0 & 0 & k_{rp1}y_{rp1} & k_{rp2}y_{rp2} & -\sum k_{rn}y_{rn} & \sum k_{rn}y^2{}_{rn} \end{bmatrix} \quad \text{(A.18)}$$

where $n = 1, 2, p1, p2$.

$$\mathbf{F}_{73}(t) = \{F_0 \sin(\omega t) \;\; M_0 \sin(\omega t) \;\; 0 \;\; 0 \;\; 0 \;\; 0\} \quad \text{(A.19)}$$

$$\mathbf{X}_{73}(t) = \{x_{3s} \;\; \theta_{3s} \;\; x_{3p1} \;\; x_{3p2} \;\; x_{3r} \;\; \theta_{3r}\} \quad \text{(A.20)}$$

Data Availability

All data included in this study are available upon request by contact with the corresponding author.

Conflicts of Interest

The authors declare that they have no conflicts of interest.

Acknowledgments

This study was supported by the National Natural Science Foundation of China (51305072).

References

[1] Z. Yimin, *Mechanical Vibration*, Tsinghua University Press, Beijing, China, 2007.

[2] Y. Jikuan, C. Min, and C. Xiaolin, "Estimate of vibration isolation effect. Noise and Vibration Control," *Noise and Vibration Control*, vol. 6, pp. 22–30, 1997.

[3] J.-B. Su, H.-C. Zhu, Z.-M. Xie, and C.-W. Su, "Acoustic source identification using partial measured data on the source surface," *Zhendong Gongcheng Xuebao*, vol. 30, no. 1, pp. 71–78, 2017.

[4] H. Feng and Q. Wang, "Vibration source identification of typical equipment," *Noise and Vibration Control*, vol. 4, no. 2, pp. 128–131, 2012.

[5] Y. Kai, Z. Yewei, C. Liqun et al., "Space structure vibration control based on passive nonlinear energy sink," *Journal of Dynamics and Control*, vol. 12, no. 3, pp. 205–208, 2014.

[6] J. Niu and K. Song, "Transmission characteristics of fully flexible isolation systems subjected to multi-excitations and supported by multi-mounts," *Jixie Gongcheng Xuebao/Journal of Mechanical Engineering*, vol. 47, no. 7, pp. 59–64, 2011.

[7] R. Singh and S. Kim, "Examination of multi-dimensional vibration isolation measures and their correlation to sound radiation over a broad frequency range," *Journal of Sound and Vibration*, vol. 262, no. 3, pp. 419–455, 2003.

[8] S. Kim and R. Singh, "Multi-dimensional characterization of vibration isolators over a wide range of frequencies," *Journal of Sound and Vibration*, vol. 245, no. 5, pp. 877–913, 2001.

[9] A. N. Thite and D. J. Thompson, "The quantification of structure-borne transmission paths by inverse methods. part 1: improved singular value rejection methods," *Journal of Sound and Vibration*, vol. 264, no. 2, pp. 411–431, 2003.

[10] A. N. Thite and D. J. Thompson, "The quantification of structure-borne transmission paths by inverse methods. Part 2: Use of regularization techniques," *Journal of Sound and Vibration*, vol. 264, no. 2, pp. 433–451, 2003.

[11] M. V. Van Der Seijs, D. De Klerk, and D. J. Rixen, "General framework for transfer path analysis: History, theory and classification of techniques," *Mechanical Systems and Signal Processing*, vol. 68-69, pp. 217–244, 2016.

[12] P. Gajdatsy, K. Janssens, W. Desmet, and H. Van Der Auweraer, "Application of the transmissibility concept in transfer path analysis," *Mechanical Systems and Signal Processing*, vol. 24, no. 7, pp. 1963–1976, 2010.

[13] D. De Klerk and A. Ossipov, "Operational transfer path analysis: Theory, guidelines and tire noise application," *Mechanical Systems and Signal Processing*, vol. 24, no. 7, pp. 1950–1962, 2010.

[14] W. Cheng, Y. Lu, and Z. Zhang, "Tikhonov regularization-based operational transfer path analysis," *Mechanical Systems and Signal Processing*, vol. 75, pp. 494–514, 2015.

[15] B.-L. Kim, J.-Y. Jung, and I.-K. Oh, "Modified transfer path analysis considering transmissibility functions for accurate estimation of vibration source," *Journal of Sound and Vibration*, vol. 398, pp. 70–83, 2017.

[16] H. Lei and Z. Jiming, "Contribution analysis of pipeline vibration based on TPA," *Chinese Ship Research*, vol. 7, no. 1, pp. 61–64, 2012.

[17] S. Meiping, "Statistical energy analysis for complicated coupled system and its application in engineering," *Engineering Science in China*, vol. 4, no. 6, pp. 77–84, 2002.

[18] S. K. Lee, "Application of vibrational power flow to a passenger car for reduction of interior noise," *Shock and Vibration*, vol. 7, no. 5, pp. 277–285, 2000.

[19] G. Feng, Y. Chen, X. Huang, and H. Hua, "Study of transmission paths in a flexible system based on power flow," *Jixie Qiangdu/Journal of Mechanical Strength*, vol. 32, no. 5, pp. 719–722, 2010.

[20] B Xiao, L Biao, and X. Chunyan, "Vibration transmission of double-layer vibration isolation system based on power flow method," *Journal of Mechanical Engineering*, vol. 47, no. 5, pp. 106–113, 2011.

[21] N. Zhenhua, *Vibration Mechanics*, Xi'an Jiao Tong University Press, Xian, China, 1989.

[22] Y. Jikuan, *Mechanical Vibration Isolation Technology*, Shanghai Science and Technology Press, Shanghai, China, 1986.

[23] Z. Shijian, L. Jingjun, H. Qiwei, and W. Xuetao, *Vibration Theory and Vibration Isolation*, National Defense Industry Press, Beijing, China, 2006.

[24] A. Inoue, R. Singh, and G. A. Fernandes, "Absolute and relative path measures in a discrete system by using two analytical methods," *Journal of Sound and Vibration*, vol. 313, no. 3-5, pp. 696–722, 2008.

[25] R. Fan and Z. Lu, "On the design method of three-point mounting system in automotive powertrain," *Automotive Engineering Magazine*, vol. 27, no. 3, pp. 304–308, 2005.

[26] L. Hai-feng, Z. Shi-jian, and L. Xue-wei, "Analysis of the effects of bearing stiffness on vibration transmission paths in ship propulsion shafting," *Noise and Vibration Control*, vol. 36, no. 1, pp. 57–60, 2016.

[27] W. Zhao and Y. Zhang, "Reliability analysis of random vibration transmission path systems," *Mechanical Systems and Signal Processing*, vol. 113, pp. 77–89, 2018.

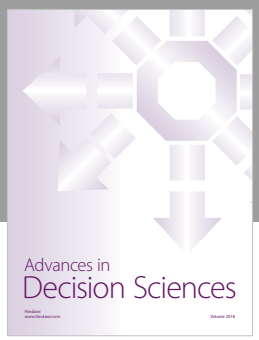

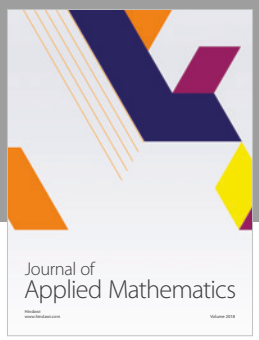

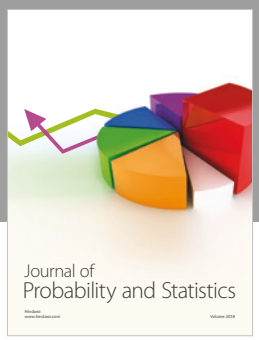

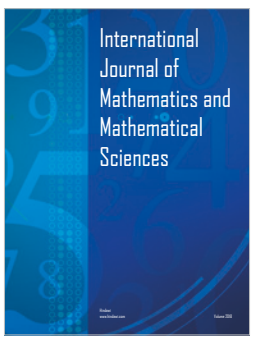

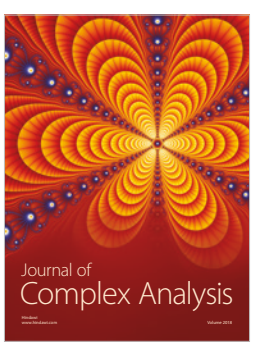

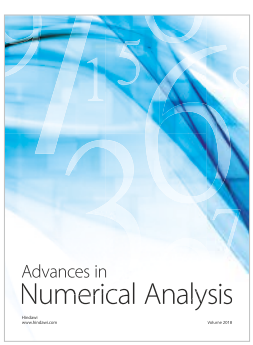

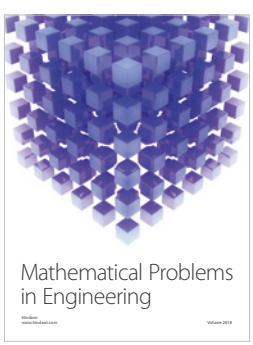

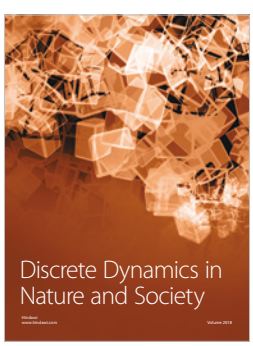

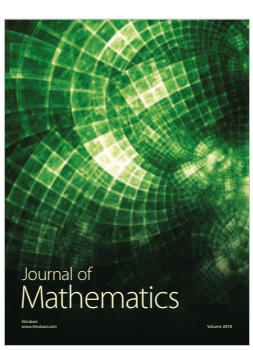

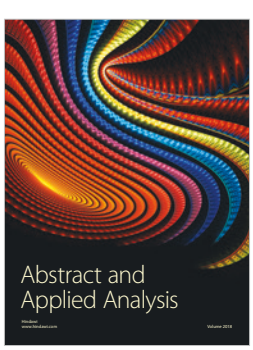

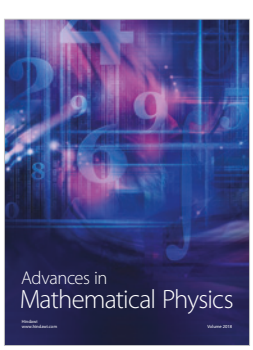

Hindawi

Submit your manuscripts at
www.hindawi.com